Pergamon

Int. J. Heat Mass Transfer. Vol. 38, No. 18, pp. 3423–3431, 1995
Copyright © 1995 Elsevier Science Ltd
Printed in Great Britain. All rights reserved
0017-9310/95 $9.50+0.00

0017-9310(95)00088-7

Evaluation of an improved hybrid six-flux/zone model for radiative transfer in rectangular enclosures

CHRISTIAN SASSE, ROLAND KOENIGSDORFF and STEFAN FRANK

German Aerospace Research Establishment (DLR), Institute of Technical Thermodynamics, Pfaffenwaldring 38-40, D-70569 Stuttgart, Germany

(*Received* 24 *October* 1994 *and in final form* 31 *January* 1995)

Abstract—An improved model for the calculation of radiative transfer in enclosures filled with an absorbing, emitting and scattering medium is presented. The model is denoted by a hybrid six-flux/zone model since it combines features of both the zone method and (three-dimensional) six-flux models. Compared to the zone method, computation time is considerably reduced and reaches approximately the same order as the faster flux-type models. The accuracy of the hybrid six-flux/zone model presented here is drastically improved without increasing computation time. This is achieved by introducing a correction for the directional characteristics of the propagation of radiation through adjacent zones. The thus improved hybrid model is evaluated for a realistic recognized test problem and found to be an efficient and accurate tool for calculating radiative transfer in enclosures filled with a participating medium.

1. INTRODUCTION

The Monte-Carlo method [1, 2] and the zone method [3] are the most rigorous methods for computing radiative transfer in enclosures filled with a participating medium, as it occurs in industrial furnaces, combustion chambers or some types of directly absorbing high temperature solar receivers [4]. Unfortunately sufficient accuracy of both calculation methods is possible only at high computational expense.

For this reason these methods are not suitable as a part of complex models where flow, reaction and heat transfer are calculated simultaneously because then computational economy is important. In those cases the faster but generally more inaccurate flux models [5, 6] are widely employed. For three-dimensional problems six-flux models based on the Schuster–Schwarzschild approach are most common [7]. They are based on six subdivisions of the 4π sr solid angle surrounding a point in the enclosure. In each subdivision the distribution of radiative intensity leaving the point is simplified to one discrete radiation flux.

In the last few years a simplified zone method was derived and applied by Scholand [8], Mehrwald [9] and Charette *et al.* [10]. This new method is characterized by good accuracy and considerably reduced computational expense, therefore it seems to be a good alternative to flux models. In the present paper a hybrid six-flux/zone model is developed which is based on this simplified zone method with the model equations being derived in the finite difference form of flux equations. The model is implemented to compute radiative transfer in rectangular enclosures filled with a grey medium. In addition to the approaches reported in refs. [8–10], scattering in the medium is taken into account. The walls of the enclosure are assumed to be grey and diffusely reflecting. The temperature distribution of the medium and the walls is assumed to be given.

Results of the hybrid model for simple test cases show that the approaches of Scholand, Mehrwald and Charette *et al.* yield incorrect computation of radiative transfer if the emission of the walls predominates over the emission of the medium, or if the number of subdivisions (zones) in the enclosure is high. It is therefore tempting to explore how radiative transfer within a single zone can be modified in order to achieve better results when computing the transfer through several zones. A simple and effective approach is presented and discussed in the present paper.

2. THE HYBRID SIX-FLUX/ZONE MODEL

The new hybrid six-flux/zone model presented here is based on subdivision of the enclosure into finite volume elements (zones) similar to the zone method. The main difference from the zone method, however, is that the hybrid model considers only radiative transfer between adjacent zones. Thus radiative transfer through the entire enclosure is calculated step by step from zone to zone, while the original zone method computes the direct interactions of all zones. Hence the computational expense of the hybrid model is reduced considerably when compared with the zone method (reduction factor of up to 24 [10]).

The hybrid model assumes imaginary planes separating the zones. The planes 'collect' the radiation which is transferred from a given zone to its neighbour and then re-emit it diffusely. In other words, the

NOMENCLATURE

A	area
b	scattering fraction backward
f	scattering fraction forward
F	configuration factor
g	weighting factor
I	radiative flux density in the x, y or z direction [W m^{-2}]
J	radiative flux density against the x, y or z direction [W m^{-2}]
N	number of zones or subdivisions
q	radiative flux density removed by a boundary [W m^{-2}]
$\dot{Q}$	transferred radiative power [W]
s	scattering fraction sideward
S	radiative source term in the medium [W m^{-3}]
T	absolute temperature in the medium or at the boundaries [K].

Greek symbols

Δ	difference
ε	emissivity of a boundary or emittance of a zone, respectively
ϑ	reception factor ($F \cdot \tau$)
ρ	reflectivity of a boundary or reflectance of a zone, respectively
σ	Stefan–Boltzmann constant [W m^{-2} K^{-4}]
τ	transmissivity of a boundary or transmittance of a zone, respectively
Ψ	function for the optimal determination of the weighting factor [W].

Subscripts

b	bottom
e	east
i,j	walls or imaginary planes, respectively (w, e, s, n, b or t)
k	kth zone
med	medium
n	north
rel	relative
s	south
t	top
w	west
x, y, z	coordinate directions
ξ	coordinate directions (x, y or z)
0	dimensionless quantity.

Superscripts

$'$	modified.

imaginary planes condense the incident flux distribution to *one* radiative flux with a perfectly diffuse characteristic, similar to some flux models [11].

The model equations of the hybrid model are derived by considering radiative transfer in one of the box-shaped zones. Such a zone is sketched in Fig. 1. The following equation describes the radiant flux transferred from one zone through the imaginary plane in the east (subscript e) into the adjacent zone.

$$
\begin{aligned}
I_e \cdot A_e = {} & \underbrace{\bar{\varepsilon}_x \cdot \sigma T^4 \cdot A_e}_{\text{term 1}} + \underbrace{F_{w,e}\bar{\tau}_{w,e} \cdot I_w A_w}_{\text{term 2}} + \underbrace{F_{s,e}\bar{\tau}_{s,e} \cdot I_s A_s}_{\text{term 3}} \\
& + \underbrace{F_{n,e}\bar{\tau}_{n,e} \cdot J_n A_n}_{\text{term 4}} + \underbrace{F_{b,e}\bar{\tau}_{b,e} \cdot I_b A_b}_{\text{term 5}} + \underbrace{F_{t,e}\bar{\tau}_{t,e} \cdot J_t A_t}_{\text{term 6}} \\
& + \underbrace{f_x \bar{\rho}_x \cdot I_w A_w}_{\text{term 7}} + \underbrace{b_x \bar{\rho}_x \cdot J_e A_e}_{\text{term 8}} + \underbrace{s_{yx}\bar{\rho}_y \cdot I_s A_s}_{\text{term 9}} \\
& + \underbrace{s_{yx}\bar{\rho}_y \cdot J_n A_n}_{\text{term 10}} + \underbrace{s_{zx}\bar{\rho}_z \cdot I_b A_b}_{\text{term 11}} + \underbrace{s_{zx}\bar{\rho}_z \cdot J_t A_t}_{\text{term 12}}. \qquad (1)
\end{aligned}
$$

Term 1 describes emission of the grey medium in the zone. T is the mean temperature of the zone and $\bar{\varepsilon}_x$ is the mean emittance of the zone through the imaginary plane in the east (positive x direction). The value of $\bar{\varepsilon}_x$ can be determined for example by the mean beam length concept [12, 13] or by a Monte-Carlo simulation of radiative transfer inside the zone [14].

Terms 2–6 describe transmission of all incoming fluxes through the zone to the imaginary plane A_e. The quantity $F_{i,j}$ is the configuration factor between the diffusely emitting plane A_i and the absorbing plane A_j, with $i, j \in \{w, e, s, n, b, t\}$ [3]. The quantity $\bar{\tau}_{i,j}$ is the mean transmittance of the zone for the radiation being transmitted from A_i to A_j. It can be determined analogous to the emittance.

Terms 7–12 consider the radiation that is scattered out of the zone through the plane A_e. The quantity $\bar{\rho}_\xi$ describes the scattered part of the radiation incident along the positive or the negative ξ direction. It can be determined by the following relationship:

$$\bar{\rho}_\xi = 1 - \bar{\varepsilon}_\xi - \bar{\tau}_\xi \quad \text{with} \quad \xi = x, y, z.$$

In this relationship $\bar{\tau}_\xi$ is the mean transmittance of the medium in the zone for radiation emitted diffusely by an imaginary plane normal to the ξ direction. [The derivation of $\bar{\tau}_\xi$ is described below in equations (23)–(25).]

The scattering fractions f (forward), b (backward) and s (sideward) define how the scattered radiation is distributed onto the different imaginary planes surrounding the zone. They depend on the phase function and the optical thickness of the medium in the zone and can be determined by Monte-Carlo simulation [15] or by approximative methods [16].

The product of the quantities $F_{i,j}$ and $\tau_{i,j}$ is abbreviated by the reception factor ($\vartheta_{i,j}$):

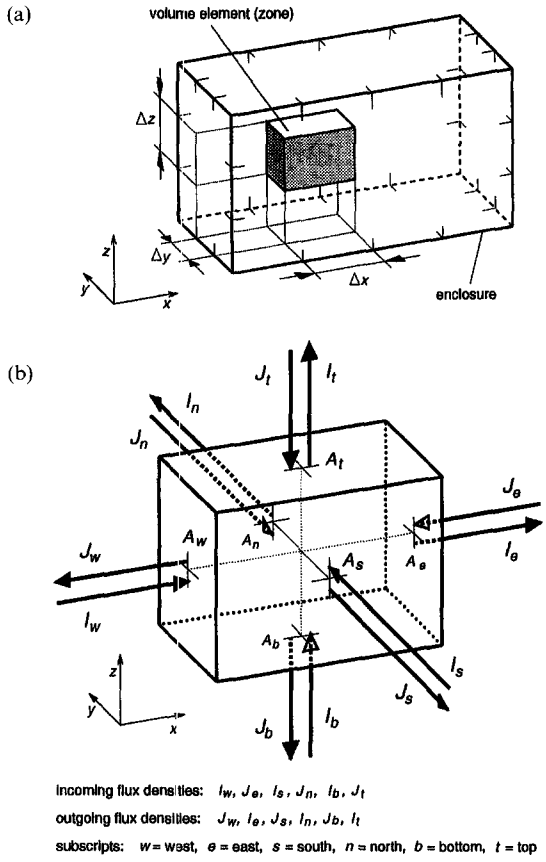

Fig. 1. (a) Subdivision of enclosure. (b) Designations of the zones.

$$\vartheta_{i,j} := F_{i,j} \cdot \bar{\tau}_{i,j} \quad \text{with} \quad i,j \in \{\mathrm{w,e,s,n,b,t}\}.$$

It is possible to simplify equation (1) by taking advantage of the symmetry of the box-shaped zone. The areas of the imaginary planes can be expressed by

$$A_\mathrm{w} = A_\mathrm{e} = \Delta y \cdot \Delta z \tag{2}$$

$$A_\mathrm{s} = A_\mathrm{n} = \Delta x \cdot \Delta z \tag{3}$$

$$A_\mathrm{b} = A_\mathrm{t} = \Delta x \cdot \Delta y \tag{4}$$

and the reception factors can be combined to

$$\vartheta_{xx} := \vartheta_{\mathrm{w,e}} = \vartheta_{\mathrm{e,w}} \tag{5}$$

$$\vartheta_{yx} := \vartheta_{\mathrm{s,e}} = \vartheta_{\mathrm{n,e}} \tag{6}$$

$$\vartheta_{zx} := \vartheta_{\mathrm{b,e}} = \vartheta_{\mathrm{t,e}}. \tag{7}$$

Dividing equation (1) by A_e and considering equations (2)–(7) results in the following equation for the outgoing flux density to the zone in the east:

$$I_\mathrm{e} = \bar{\varepsilon}_x \cdot \sigma T^4 + (\vartheta_{xx} + f_x \bar{\rho}_x) \cdot I_\mathrm{w} + b_x \bar{\rho}_x \cdot J_\mathrm{e} + (\vartheta_{yx} + s_{yx} \bar{\rho}_y) \frac{\Delta x}{\Delta y} \cdot (I_\mathrm{s} + J_\mathrm{n}) + (\vartheta_{zx} + s_{zx} \bar{\rho}_z) \frac{\Delta x}{\Delta z} \cdot (I_\mathrm{b} + J_\mathrm{t}). \tag{8}$$

Cyclic exchange of x, y and z leads to analogous relationships for the other outgoing flux densities:

$$J_\mathrm{w} = \bar{\varepsilon}_x \cdot \sigma T^4 + (\vartheta_{xx} + f_x \bar{\rho}_x) \cdot J_\mathrm{e} + b_x \bar{\rho}_x \cdot I_\mathrm{w} + (\vartheta_{yx} + s_{yx} \bar{\rho}_y) \frac{\Delta x}{\Delta y} \cdot (I_\mathrm{s} + J_\mathrm{n}) + (\vartheta_{zx} + s_{zx} \bar{\rho}_z) \frac{\Delta x}{\Delta z} \cdot (I_\mathrm{b} + J_\mathrm{t}) \tag{9}$$

$$I_\mathrm{n} = \bar{\varepsilon}_y \cdot \sigma T^4 + (\vartheta_{yy} + f_y \bar{\rho}_y) \cdot I_\mathrm{s} + b_y \bar{\rho}_y \cdot J_\mathrm{n} + (\vartheta_{xy} + s_{xy} \bar{\rho}_x) \frac{\Delta y}{\Delta x} \cdot (I_\mathrm{w} + J_\mathrm{e}) + (\vartheta_{zy} + s_{zy} \bar{\rho}_y) \frac{\Delta y}{\Delta z} \cdot (I_\mathrm{b} + J_\mathrm{t}) \tag{10}$$

$$J_\mathrm{s} = \bar{\varepsilon}_y \cdot \sigma T^4 + (\vartheta_{yy} + f_y \bar{\rho}_y) \cdot J_\mathrm{n} + b_y \bar{\rho}_y \cdot I_\mathrm{s} + (\vartheta_{xy} + s_{xy} \bar{\rho}_x) \frac{\Delta y}{\Delta x} \cdot (I_\mathrm{w} + J_\mathrm{e}) + (\vartheta_{zy} + s_{zy} \bar{\rho}_y) \frac{\Delta y}{\Delta z} \cdot (I_\mathrm{b} + J_\mathrm{t}) \tag{11}$$

$$I_\mathrm{t} = \bar{\varepsilon}_z \cdot \sigma T^4 + (\vartheta_{zz} + f_z \bar{\rho}_z) \cdot I_\mathrm{b} + b_z \bar{\rho}_z \cdot J_\mathrm{t} + (\vartheta_{xz} + s_{xz} \bar{\rho}_x) \frac{\Delta z}{\Delta x} \cdot (I_\mathrm{w} + J_\mathrm{e}) + (\vartheta_{yz} + s_{yz} \bar{\rho}_y) \frac{\Delta z}{\Delta y} \cdot (I_\mathrm{s} + J_\mathrm{n}) \tag{12}$$

$$J_\mathrm{b} = \bar{\varepsilon}_z \cdot \sigma T^4 + (\vartheta_{zz} + f_z \bar{\rho}_z) \cdot J_\mathrm{t} + b_z \bar{\rho}_z \cdot I_\mathrm{b} + (\vartheta_{xz} + s_{xz} \bar{\rho}_x) \frac{\Delta z}{\Delta x} \cdot (I_\mathrm{w} + J_\mathrm{e}) + (\vartheta_{yz} + s_{yz} \bar{\rho}_y) \frac{\Delta z}{\Delta y} \cdot (I_\mathrm{s} + J_\mathrm{n}). \tag{13}$$

Equations (8)–(13) describe in each zone a system of six relationships that contain 12 unknown flux densities. The number of unknowns can be reduced to six per zone by considering the identity of outgoing and incoming flux densities of adjacent zones and by formulating boundary conditions for those zones that are in contact with the walls of the enclosure. These boundary conditions are:

$$I_i = \varepsilon_i \cdot \sigma T^4 + \rho_i \cdot J_i \quad \text{for} \quad i = \mathrm{w,s,b} \tag{14}$$

and

$$J_i = \varepsilon_i \cdot \sigma T^4 + \rho_i \cdot I_i \quad \text{for} \quad i = \mathrm{e,n,t} \tag{15}$$

where i is the subscript of the wall in contact with the zone, and T, ε_i and ρ_i are the mean temperature, emissivity and reflectivity of the wall.

First investigations with simple test problems showed that the hybrid model described above yields better results than common six-flux models only in some cases, and that its deviation from the exact solution increases with the number of subdivisions in the

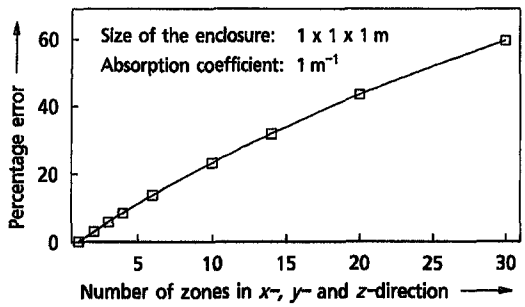

Fig. 2. Effect of the number of zones on the error predicted by the unmodified hybrid model when computing the radiative transfer from one emitting wall to the absorbing medium in a cubic enclosure.

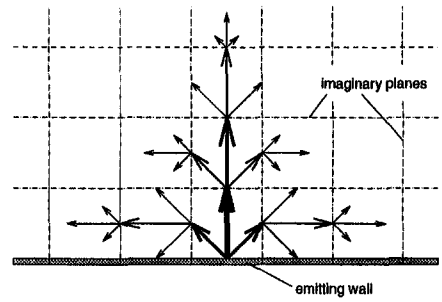

Fig. 4. Radiative transport for the modified hybrid model ($g \approx 0.5$) for an emitting wall. (The size of the arrows corresponds to the transferred radiative flux.)

enclosure [14]. An example is shown in Fig. 2. The test problem considered here is a cubic enclosure filled with an absorbing medium, surrounded by black walls and subdivided into a variable number of cubic zones. Figure 2 displays the error produced by the hybrid model when computing the radiative transfer from one emitting wall to the absorbing medium.

3. IMPROVEMENTS OF THE MODEL

A closer look at the mechanism of radiative transfer implemented in the hybrid model shows the reason for those inaccuracies. The radiation transferred between two zones is modelled by assuming perfectly diffuse re-emittance of the radiation reaching an imaginary plane, thus information about the directional distribution of the radiation is lost. As shown in Fig. 3, this loss of information leads to ray paths which do not correspond with reality. For example, part of the radiation emitted by a plain wall is turned back to the wall, even if there is no scattering in the medium. Altogether the transport of radiation through the enclosure results in many directional changes, thus elongating the path lengths in the medium artificially.

To improve the model, we suggest modifying the exchange of radiation inside the zones by emphasizing radiative transfer to the opposite imaginary plane and reducing transfer to the adjacent planes. In order to achieve this, the reception factors between opposite

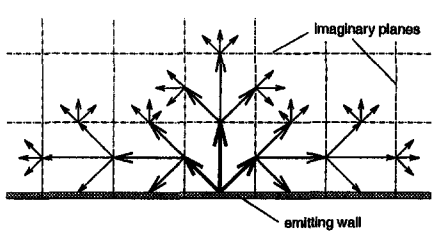

Fig. 3. Radiative transport for the hybrid model for an emitting wall. (The size of the arrows corresponds to the transferred radiative flux.)

planes $\vartheta_{\xi\xi}$ are replaced by $\vartheta'_{\xi\xi}$, utilizing the following definition in which $g \in [0, 1]$ is a weighting factor:

$$\vartheta'_{\xi\xi} := g \cdot \bar{\tau}_\xi + (1-g) \cdot \vartheta_{\xi\xi} \quad \text{with } \xi = x, y, z. \tag{16}$$

The new reception factors between adjacent planes are defined as function of $\vartheta'_{\xi\xi}$:

$$\vartheta'_{xy} := \tfrac{1}{2} \cdot \frac{\vartheta_{xy}}{\vartheta_{xy}+\vartheta_{xz}} \cdot (\bar{\tau}_x - \vartheta'_{xx}) \tag{17}$$

$$\vartheta'_{xz} := \tfrac{1}{2} \cdot \frac{\vartheta_{xz}}{\vartheta_{xy}+\vartheta_{xz}} \cdot (\bar{\tau}_x - \vartheta'_{xx}) \tag{18}$$

$$\vartheta'_{yx} := \tfrac{1}{2} \cdot \frac{\vartheta_{yx}}{\vartheta_{yx}+\vartheta_{yz}} \cdot (\bar{\tau}_y - \vartheta'_{yy}) \tag{19}$$

$$\vartheta'_{yz} := \tfrac{1}{2} \cdot \frac{\vartheta_{yz}}{\vartheta_{yx}+\vartheta_{yz}} \cdot (\bar{\tau}_y - \vartheta'_{yy}) \tag{20}$$

$$\vartheta'_{zx} := \tfrac{1}{2} \cdot \frac{\vartheta_{zx}}{\vartheta_{zx}+\vartheta_{zy}} \cdot (\bar{\tau}_z - \vartheta'_{zz}) \tag{21}$$

$$\vartheta'_{zy} := \tfrac{1}{2} \cdot \frac{\vartheta_{zy}}{\vartheta_{zx}+\vartheta_{zy}} \cdot (\bar{\tau}_z - \vartheta'_{zz}) \tag{22}$$

with

$$\bar{\tau}_x = \vartheta_{xx} + 2\vartheta_{xy} + 2\vartheta_{xz} \tag{23}$$

$$\bar{\tau}_y = \vartheta_{yy} + 2\vartheta_{yx} + 2\vartheta_{yz} \tag{24}$$

$$\bar{\tau}_z = \vartheta_{zz} + 2\vartheta_{zx} + 2\vartheta_{zy}. \tag{25}$$

The definitions (16)–(22) ensure that the total transmission through a zone is not influenced by the weighting factor g, i.e. $\bar{\tau}'_\xi = \bar{\tau}_\xi$ for $\xi = x, y, z$. The definitions also guarantee that the ratios between the reception factors to adjacent planes ($\vartheta'_{xy}/\vartheta'_{xz}$, $\vartheta'_{yx}/\vartheta'_{yz}$ and $\vartheta'_{zx}/\vartheta'_{zy}$) are independent of g. Figure 4 demonstrates the effect of these modifications on the directional characteristic of the propagation of radiation through several zones. It can be seen that the quantity of radiation returning to the emitting wall is reduced and that the radiation is led more directly through the medium which corresponds better to reality. In the extreme case of $g = 1$ the transmitted radiation is directed only forwards to the opposite imaginary plane of a zone. In this case the hybrid model behaves like a six-flux model.

In order to determine the best value for g, we utilized the following procedure: radiative transfer was determined with the hybrid model in an enclosure of similar size, subdivision and optical properties as in the real problem. Since the temperature distribution in the enclosure is generally unknown, we assumed the medium to be at a uniform temperature (e.g. 1000 K) and the surrounding walls to be at 0 K. The total radiative power transferred from the medium to the walls was computed for several values of the weighting factor g and compared with reference results from the zone method or Monte-Carlo simulation. The value of g for which the hybrid model matched the reference case best was then chosen as the weighting factor in order to calculate the real problem. The following function was applied as a criterion for this optimization problem:

$$\Psi(g) = |\Delta\dot{Q}_{\text{med}}(g)| + \sum_j |\Delta\dot{Q}_j(g)| \quad \text{for} \quad j = \text{w, e, s, n, b and t} \qquad (26)$$

where $\Delta\dot{Q}_{\text{med}}$ is the difference between the model prediction of net emission of the entire medium and the reference solution and $\Delta\dot{Q}_j$ is the difference between the model prediction of absorption of one entire wall (j) and the reference solution.

For the test problem described below function (26) reaches a minimal value for $g = 0.51$. The value of g increases if the number of subdivisions of the enclosure is also increased. It decreases for increasing optical thickness in the enclosure [14].

4. THE TEST PROBLEM

In order to assess the quality of the hybrid model, a realistic test problem is chosen as suggested and used by Selçuk in refs. [17, 18]. The test problem is based on data Strömberg gathered in a large scale experimental furnace with steep temperature gradients, as they are typical for industrial furnaces [19]. The box-shaped experimental furnace has a size of $0.96 \times 0.96 \times 5.76$ m in the x, y and z directions, respectively. The exact solution of radiative heat transfer was calculated by Selçuk with the following assumptions [17]:

1. The furnace is assumed as an enclosure with black walls, filled with a grey, emitting and absorbing medium.
2. The absorption coefficient of the medium is constant throughout the enclosure.
3. The temperature distribution of the enclosure is symmetrical with respect to the longitudinal axis (z-axis) of the furnace.
4. The enclosure is subdivided into $4 \times 4 \times 24$ cubic zones.

Selçuk computed the exact solution by using dimensionless quantities; for details see ref. [17].

5. ACCURACY

Selçuk used the test problem described above to evaluate a new six-flux model developed by her with Siddall. Results are compared with a six-term discrete ordinate model and a simpler six-flux model of the Schuster–Schwarzschild type [18]. The evaluation shows considerable improvements in accuracy and less computational expense of their model in comparison with the other models. This is achieved by the good adaptation of the new model to the geometry of the problem by using variable subdivision of the 4π sr solid angle. In the present paper the following models are used to evaluate the improved hybrid six-flux zone model:

1. The six-flux model of Selçuk and Siddall [6], shown to be most accurate for the test problem investigated by Selçuk [18].
2. The hybrid six-flux/zone model without modification of radiative exchange inside the zones ($g = 0$), which is equivalent to the approaches of Mehrwald [9] and Charette *et al.* [10].
3. The hybrid six-flux/zone model with a modified radiative exchange inside the zones ($g = 0.51$) as described above.

Figures 5–7 show the distribution of the dimensionless radiative source term predicted by the different models in comparison with the exact solution. The distribution is plotted in three rows parallel to the z-axis of the furnace. The source terms predicted by the Selçuk/Siddall model match the exact solution for the inner row of the medium (Fig. 5), but there are some differences for the corner row and the middle row (Figs. 6 and 7).

The source terms are underpredicted by about 10% for the hybrid model with $g = 0$ (no modification). This is due to the overprediction of radiative path length in the medium discussed earlier which results in higher reabsorption of emitted radiation in the medium. Figures 5–7 show that this error is drastically reduced by emphasizing the forward direction in the radiative exchange within the zones: in all three rows the prediction of the modified hybrid model with $g = 0.51$ corresponds well with the exact solution.

When considering the flux density removed by the side walls (Figs. 8 and 9), the values predicted by the hybrid model match the exact solution better than the Selçuk/Siddall model in both cases, $g = 0$ and $g = 0.51$. This can be confirmed by computing the average deviation of the predicted values from the exact solution as shown in Table 1. The values in Table 1 are related to the mean source term of the medium or the mean flux density at the side walls, respectively:

$$\overline{\Delta S}_{\text{rel}} = \frac{\frac{1}{N_{\text{med}}} \sum_{k=1}^{N_{\text{med}}} |S_{\text{model},k} - S_{\text{exact},k}|}{\frac{1}{N_{\text{med}}} \sum_{k=1}^{N_{\text{med}}} S_{\text{exact},k}} \qquad (27)$$

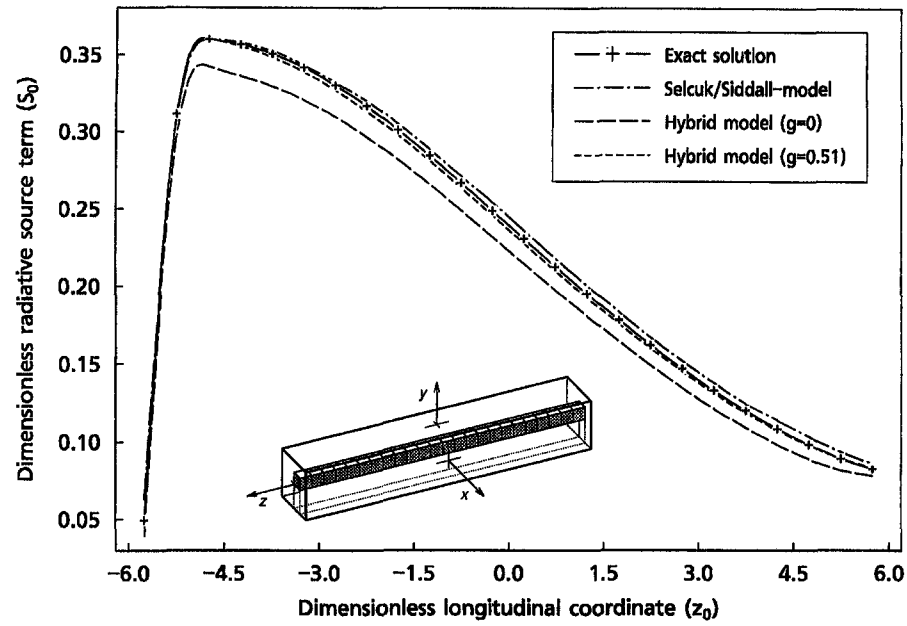

Fig. 5. Comparison between exact values and model predictions (inner row of medium: $x_0 = 0.25$, $y_0 = 0.25$).

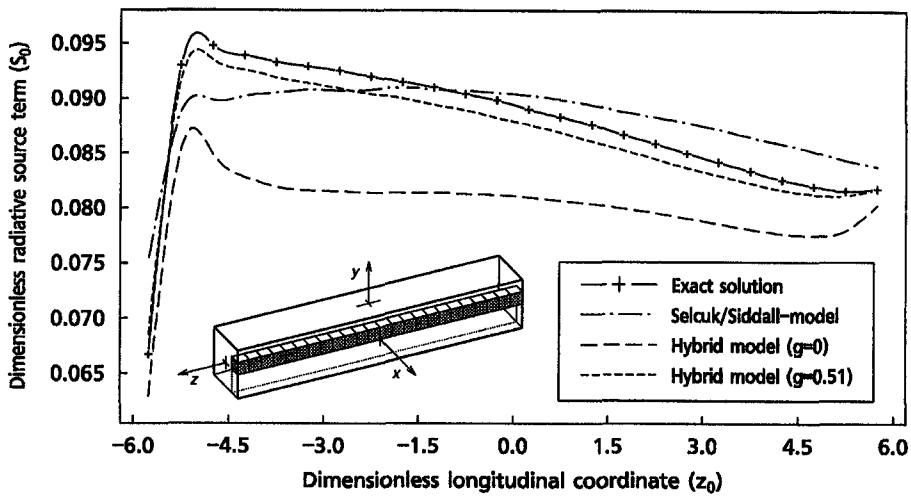

Fig. 6. Comparison between exact values and model predictions (middle row of medium: $x_0 = 0.75$, $y_0 = 0.25$).

Table 1. Average deviation of model predictions from exact solution for source terms (S) and flux densities (q)

Model	Average deviation in the medium, $\overline{\Delta S_{rel}}$ [%]	Average deviation at the longitudinal walls, $\overline{\Delta q_{rel}}$ [%]
Selçuk/Siddall model	2.7	18.1
Hybrid model ($g = 0$)	6.7	8.4
Hybrid model ($g = 0.51$)	1.1	7.3
Hybrid model ($g = 0.47$)	1.3	7.0
Hybrid model ($g = 0.55$)	0.9	7.8

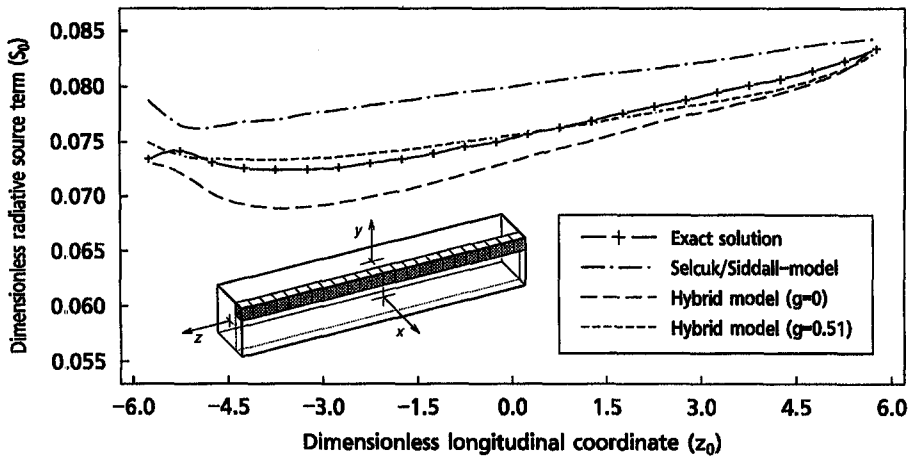

Fig. 7. Comparison between exact values and model predictions (corner row of medium: $x_0 = 0.75$, $y_0 = 0.75$).

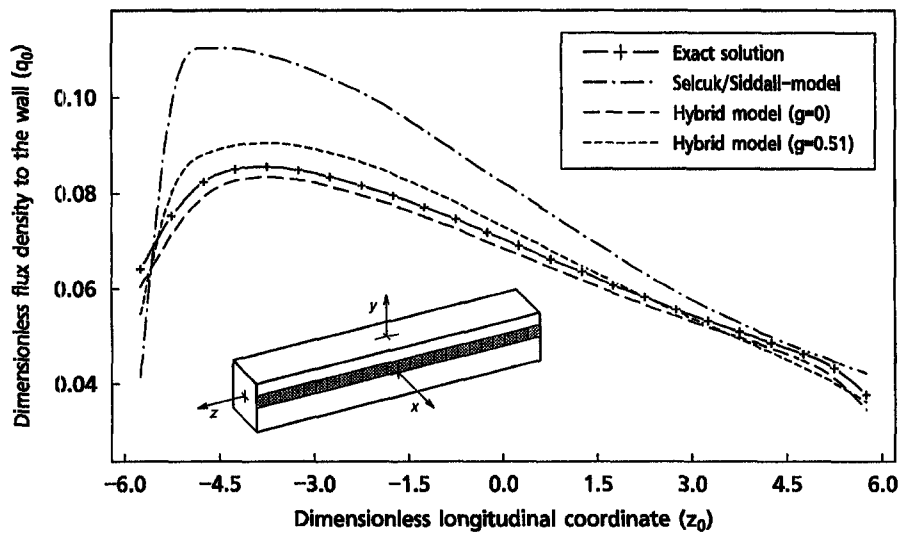

Fig. 8. Comparison between exact values and model predictions (inner row of wall: $x_0 = 1.0$, $y_0 = 0.25$).

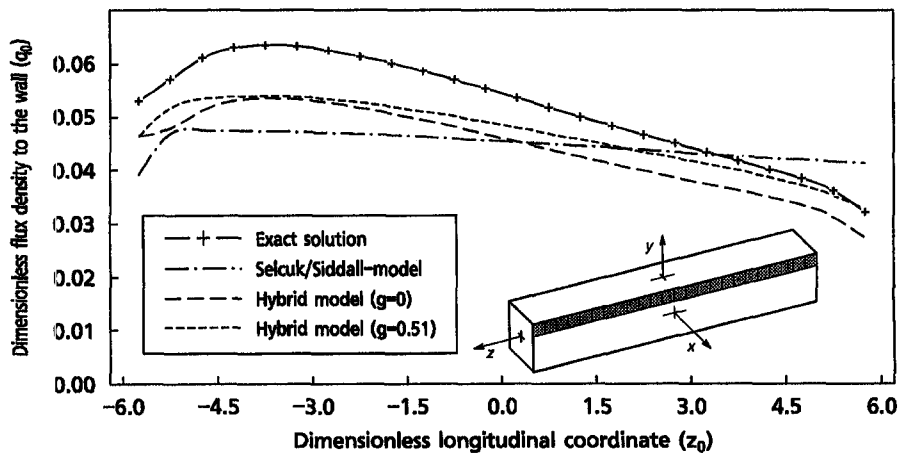

Fig. 9. Comparison between exact values and model predictions (corner row of wall: $x_0 = 1.0$, $y_0 = 0.75$).

$$\overline{\Delta q_{\mathrm{rel}}} = \frac{\frac{1}{N_{\mathrm{wall}}} \sum_{k=1}^{N_{\mathrm{wall}}} |q_{\mathrm{model},k} - q_{\mathrm{exact},k}|}{\frac{1}{N_{\mathrm{wall}}} \sum_{k=1}^{N_{\mathrm{wall}}} q_{\mathrm{exact},k}}$$

where N_{med} is the number of zones in the medium and N_{wall} is the number of subdivisions at the longitudinal walls.

From Table 1 it can be concluded that the modified hybrid model ($g = 0.51$) is considerably more accurate than the Selçuk/Siddall model or the unmodified hybrid model ($g = 0$). Table 1 shows also that good accuracy is still given for values of g between 0.47 and 0.55. Thus exact determination of the weighting factor is not essential to yield good results, which facilitates practical application.

Further tests where optical depth, temperature distribution and the number of subdivisions in the furnace were varied also proved sufficient accuracy of the hybrid model. This was confirmed by results of a second test problem, in which radiative transfer in a particle receiver for concentrated solar radiation [11] was calculated [14]. This problem also included scattering in the medium. Results from Monte-Carlo simulations were used as reference in those tests and the hybrid model was compared with a simple six-flux model based on equal subdivisions of the solid angle around a given point in the medium described in ref. [11].

6. COMPUTATIONAL EXPENSE

As can be seen from Table 1, the modified hybrid model is a good alternative to the six-flux models; but for most applications computational expense is at least as important as accuracy. In Table 2 the computational expense of the hybrid model is compared with the fastest six-flux model in the evaluation carried out by Selçuk [18]. The values in Table 2 show the number of iteration steps required to solve the system of linear equations resulting from six-flux models or hybrid models for the test problem. The iteration was terminated as soon as computed flux values in all grid points differed by less than 0.0001% from the values obtained in the previous iteration step [18].

Unfortunately, the numerical solution procedure used for the hybrid model is not identical to the one used for the six-flux model in ref. [18]. The solution of the hybrid model is based on the Gauß–Seidel algorithm [20]. Six-flux models can take advantage of their tri-diagonal type coefficient matrix, resulting in a reduced number of iteration steps. On the other hand, they need more computing time per iteration step than the Gauß–Seidel algorithm, thus computing time required to compute radiative transfer in the furnace with both models is about the same [14].

Table 2. Comparison of computational expense for the different models applied to the test problem

Model	Number of iteration steps
Selçuk/Siddall model	9
Hybrid model ($g = 0$)	28
Hybrid model ($g = 0.51$)	14

7. CONCLUSION

In this paper an improved hybrid six-flux/zone model for the calculation of radiative transfer in enclosures filled with a participating medium has been presented. In continuation of previous approaches, the directional distribution of the radiation at the imaginary planes separating the zones is modified. The modification is controlled by a weighting factor.

The importance of modifying the directional distribution was demonstrated for a realistic test problem. Considerably improved accuracy in comparison with the unmodified hybrid model or with six-flux models was achieved. Furthermore, computational expense of the hybrid model was found to be comparable with conventional flux models and thus much lower than the expense of the zone method, therefore the modified hybrid model developed here represents considerable progress on the path to fast and highly accurate models for calculating radiative transfer.

REFERENCES

1. R. Siegel and J. R. Howell, *Thermal Radiation Heat Transfer* (2nd Edn), Chaps 11 and 20. Hemisphere, New York (1981).
2. C. V. S. Murty, Evaluation of reception factors in a rotary kiln using a modified Monte-Carlo scheme, *Int. J. Heat Mass Transfer* **36**, 119–133 (1993).
3. H. C. Hottel and A. F. Sarofim, *Radiative Transfer*. McGraw-Hill, New York (1967).
4. R. Koenigsdorff, *Direkteinkopplung konzentrierter Solarstrahlung in eine zirkulierende Wirbelschicht*, VDI Fortschritt-Berichte, Reihe 6, Nr. 301. VDI-Verlag, Düsseldorf, Germany (1994).
5. A. G. de Marco and F. C. Lockwood, A new flux model for the calculation of radiation in furnaces, *Riv. Combust.* **29**, 184–196 (1975).
6. R. G. Siddall and N. Selçuk, Evaluation of a new six-flux model for radiative transfer in rectangular enclosures, *Trans. Inst. Chem. Engrs* **57**, 163–169 (1979).
7. K. Görner, *Technische Verbrennungssysteme*. Springer, Heidelberg (1991).
8. E. Scholand, *A Simple Mathematical Model to Predict the Radiant Heat Transfer in Combustion Chambers* (in German), VDI Fortschritt-Berichte, Reihe 6, No. 111. VDI-Verlag, Düsseldorf, Germany (1982).
9. A. Mehrwald, Mathematische Simulation und meßtechnische Untersuchung des Einflusses der Rezirkulation von Abgas auf die Wärmeübertragung und Schadstoffbildung in einer Umkehrbrennkammer, Ph.D. Thesis, Ruhr-Universität, Bochum, Germany (1991).
10. A. Charette, A. Larouche and Y. S. Kocaefe, Application of the imaginary planes method to three-dimensional systems, *Int. J. Heat Mass Transfer* **33**, 2671–2681 (1990).
11. F. Miller and R. Koenigsdorff, Thermal modelling of a small-particle solar central receiver, submitted to *J. Solar Energy Engng*.

12. R. Siegel and J. R. Howell, *Thermal Radiation Heat Transfer* (2nd Edn), Chap. 17. Hemisphere, New York (1981).
13. W. W. Yuen and A. Ma, Evaluation of total emittance of an isothermal nongray absorbing scattering gas-particle mixture based on the concept of absorption mean beam length, *ASME J. Heat Transfer* **114,** 653–658 (1992).
14. S. Frank, Formulierung und Test eines hybriden Sechs-Fluß/Zonen-Modells zur Berechnung des Strahlungsaustausches in Gas-Partikel-Gemischen, M.Sc. Thesis, Institute für Thermodynamik und Wärmetechnik der Universität Stuttgart and Institut für Technische Thermodynamik der DLR, Stuttgart, Germany (1994).
15. C. Sasse, Determination of the optical properties of particles for solar heated fluidized beds, Ph.D. Thesis (in German), Universität Karlsruhe, DLR-FB 92-15, Germany (1992).
16. R. Koenigsdorff, F. Miller and R. Ziegler, Calculation of scattering fractions for use in radiative flux models, *Int. J. Heat Mass Transfer* **34,** 2673–2676 (1991).
17. N. Selçuk, Exact solutions for radiative heat transfer in box-shaped furnaces, *ASME J. Heat Transfer* **107,** 648–655 (1985).
18. N. Selçuk, Evaluation of flux models for radiative transfer in rectangular furnaces, *Int. J. Heat Mass Transfer* **31,** 1477–1482 (1988).
19. L. Strömberg, Calculation of heat flux distribution in furnaces, Ph.D. Thesis, Chalmars University of Technology, Gotheburg, Sweden (1977).
20. V. Patankar Suhas, *Numerical Heat Transfer and Fluid Flow*, Chap. 4.4. McGraw-Hill, London (1980).